Journal of Applied Statistics
Publication details, including instructions for authors and subscription information:
http://www.tandfonline.com/loi/cjas20

Extreme value and cluster analysis of European daily temperature series

Manuel G. Scotto [a], Susana M. Barbosa [b] & Andrés M. Alonso [c]

[a] Departamento de Matemática, Universidade de Aveiro, Portugal

[b] Instituto Dom Luiz, Universidade de Lisboa, Portugal

[c] Departamento de Estadística, Instituto Flores de Lemus, Universidad Carlos III de Madrid, Spain

Available online: 24 Jun 2011

Journal of Applied Statistics
Vol. 38, No. 12, December 2011, 2793–2804

Extreme value and cluster analysis of European daily temperature series

Manuel G. Scotto[a]*, Susana M. Barbosa[b] and Andrés M. Alonso[c]

[a] *Departamento de Matemática, Universidade de Aveiro, Portugal;* [b] *Instituto Dom Luiz, Universidade de Lisboa, Portugal;* [c] *Departamento de Estadística, Instituto Flores de Lemus, Universidad Carlos III de Madrid, Spain*

(*Received 24 April 2010; final version received 7 March 2011*)

Time series of daily mean temperature obtained from the European Climate Assessment data set is analyzed with respect to their extremal properties. A time-series clustering approach which combines Bayesian methodology, extreme value theory and classification techniques is adopted for the analysis of the regional variability of temperature extremes. The daily mean temperature records are clustered on the basis of their corresponding predictive distributions for 25-, 50- and 100-year return values. The results of the cluster analysis show a clear distinction between the highest altitude stations, for which the return values are lowest, and the remaining stations. Furthermore, a clear distinction is also found between the northernmost stations in Scandinavia and the stations in central and southern Europe. This spatial structure of the return period distributions for 25-, 50- and 100-years seems to be consistent with projected changes in the variability of temperature extremes over Europe pointing to a different behavior in central Europe than in northern Europe and the Mediterranean area, possibly related to the effect of soil moisture and land-atmosphere coupling.

Keywords: daily mean temperature series; cluster analysis; Bayesian inference; return values

1. Introduction

Extremes values of climate parameters can have profound societal impacts, affecting human health, energy use, agriculture, water resources and ecosystems [24,28,38]. For example, in the case of temperature, heat waves are associated with increasing mortality rates in human populations [2], the depletion of water resources [18,14], the reduction in vegetation growth [17,44] and the increase in the number of forest fires [40].

Climate change is expected to affect extreme weather events. For example, heat waves are expected to become longer, more intense and more frequent [3,4,30,35]. It is well known that even a simple shift in the mean of a climate variable can have a considerable influence in the frequency of occurrence of events considered as extreme in light of the historical record [41]. Furthermore, the variability of extreme events in a warming world can differ from the variability in the mean,

*Corresponding author. Email: mscotto@ua.pt

ISSN 0266-4763 print/ISSN 1360-0532 online

http://dx.doi.org/10.1080/02664763.2011.570317
http://www.tandfonline.com

due to changes in the shape of the probability density function of a climate parameter [19]. The study of extreme values is therefore of particular relevance in a climate change context.

In this work, extreme value theory (hereafter EVT) is applied to the analysis of European daily temperature records. The analysis of extreme values implies focussing on the tails of the data distribution; therefore, it is preferable to characterize the tail of the distribution by means of EVT than to fit a distribution to the complete data [9]. However, comparatively few studies [26,27] have focussed on the EVT analysis of daily temperatures. Most studies addressed instead the temporal evolution of universally accepted indices of temperature extremes either from historical observations [1,16,21,29] or model data [8,37]. These indices usually represent return periods of the order of some weeks, and therefore describe 'moderate' extremes, since trends on more extreme values would be computed from fewer data and therefore would be more difficult to detect [21]. The analysis of the temporal evolution of extreme temperatures indices showed significant trends over Europe, particularly in extreme warm events [21,25,39].

The spatial distribution of extreme events is of both physical and practical interest, particularly in the case of regional studies. Characterization of spatial extremes has become an important topic of research in the last years [6,10,20]. A common feature of the previous works, however, is that all of them rely on a likelihood-based approach. Recently, Bayesian hierarchical models for spatial extremes have been proposed. For example, Cooley *et al*. [11] introduced a Bayesian hierarchical model in which locally the extreme rainfall is modeled by a one-dimensional EVT distribution and the parameters of this distribution follow some spatial dependence model. Extensions of this model have been recently proposed by Sang and Gelfand [33,34].

On the other hand, approaches for addressing spatial features of extreme temperatures often consider each time series individually, summarizing the information for the region of interest in terms of maps of individual features [7,21]. An alternative approach is to consider cluster analysis for assessing the spatial distribution of temperature extremes [32]. In the present study, a Bayesian extreme value analysis is combined with a time series clustering procedure for describing regional extreme temperature variability over Europe.

The rest of the paper is organized as follows. Section 2 briefly introduces basic concepts related to EVT and Bayesian methodology for extreme value models. Furthermore, the time series clustering procedure is also described. In Section 3, an application of this approach for clustering time series of daily mean temperature obtained from the European Climate Assessment (hereafter ECA) data set based on long-term predictions of extreme values is presented. Finally, some concluding remarks are given in Section 4.

2. Methods

2.1 *Extreme value approach*

EVT provides a very flexible approach for estimating the probabilities of future extremal air temperatures given historical data. The celebrated *Fisher–Tippett extreme value theorem* states that if the distribution of partial maxima of an independent and identically distributed sequence of random variables with common (unknown) distribution F, say, $M_n := \max(X_1, \dots, X_n)$, properly normalized, converges to a non-degenerate limit distribution G, i.e.

$$\lim_{n\to\infty} P\{a_n^{-1}(M_n - b_n) \leq x\} = G(x), \tag{1}$$

for some constants $a_n > 0$ and $b_n \in \mathbb{R}$, then F is in the domain of attraction of G, and G must be the *generalized extreme value* (GEV in short) distribution

$$G(x) = G_\xi(x) := \exp\left\{-\left[1 + \xi\left(\frac{x-\mu}{\sigma}\right)\right]^{-1/\xi}\right\}, \tag{2}$$

defined on $\{x : 1 + \xi(x - \mu)/\sigma > 0\}$ where $-\infty < \mu < \infty$, $\sigma > 0$ and $-\infty < \xi < \infty$. It has three parameters, μ, σ and ξ, denoting location, scale and shape parameters, respectively. The shape parameter ξ, also called the tail index, determines the three extreme value types. Specifically, when ξ takes negative values, positives values or when $\xi = 0$, interpreted by taking the limit of Equation (2) as $\xi \to 0$, the GEV distribution is the negative Weibull, the Fréchet or the Gumbel distribution, respectively. The Fréchet domain of attraction embraces heavy-tailed distributions with polynomially decaying tails. All d.f.'s belonging to the Weibull domain of attraction are light-tailed with finite right endpoint. The intermediate case $\xi = 0$ is of particular interest since this class includes distribution functions with very different tails, ranging from moderately heavy (such as the lognormal distribution) to light (such as the Normal distribution) having finite right endpoint or not.

A useful parameter of interest in many extreme value studies is the quantile x_p for a specified exceedance probability p, defined as

$$x_p := \begin{cases} \mu - \dfrac{\sigma}{\xi}\{1 - (-\log(1-p))^{-\xi}\}, & \xi \neq 0 \\ \mu - \sigma \log\{-\log(1-p)\}, & \xi = 0 \end{cases}$$

where $G(x_p) = 1 - p$. Roughly speaking, x_p is the return level that is associated with the return period $1/p$ for small p, in units of, say, years, if the GEV corresponds to the annual maximum.

A typical application in EVT is the r-largest order statistic model which consists in fitting the GEV distribution to the r-largest observations within a block, for example, a year. Note that the case $r = 1$ correspond to the well-known annual maxima method. For the asymptotic arguments to hold, the number of order statistics, r, used in each year must be chosen carefully since small values of it will produce likelihood estimators with high variance, whereas large values of r are likely to violate the asymptotic support for the model, leading to bias. In practice, it is usual to select r as large as possible subject to adequate model diagnostics. The validity of the models was checked through the application of graphical methods, in particular, the probability plot, the quantile plot and the return level plot; for further details, see [31] and references therein.

An alternative approach when dealing with extreme values is to consider a Bayesian approach. Roughly speaking, Bayes' theorem converts a prior distribution, say $\pi(\boldsymbol{\theta})$, for a parameter vector $\boldsymbol{\theta} := (\theta_1, \ldots, \theta_p)$, on the availability of historical data $\boldsymbol{x} := (x_1, \ldots, x_n)$, into a posterior distribution $\pi(\boldsymbol{\theta}|\boldsymbol{x}) \propto L(\boldsymbol{x}|\boldsymbol{\theta})\pi(\boldsymbol{\theta})$, where $L(\boldsymbol{x}|\boldsymbol{\theta})$ denotes the likelihood for the historical data. The prior expresses the degree of certainty concerning the situation before the data are taken. Hence, Bayes' theorem provides the means for updating our knowledge, expressed in terms of a probability density function, in light of some new information similarly expressed. It is important to stress the fact that the outcome of a Bayesian analysis is an entire distribution on $\boldsymbol{\theta}$, which represents a considerable advantage over classical methods; rather than just a point estimate, we obtain a complete probabilistic distribution on the parameter values. Point estimates can be easily obtained by taking the mean or the median of the posterior distribution.

2.2 *Clustering time series*

A time-series clustering procedure based on long-term predictions of extreme values of temperature records is applied in the present study to describe the regional temperature variability in Europe. We only outline here the essential of the method referring the reader to the work of Scotto *et al.* [36] and the references therein for a more detailed description.

Our starting point is a panel of T time series $\mathbf{X} := (\mathbf{X}^{(1)}, \ldots, \mathbf{X}^{(T)})$ observed for, say $n_1, \ldots, n_T$, time units, respectively, that is, $\mathbf{X}^{(i)} := (X_{1,i}, \ldots, X_{n_i,i})$ for $i = 1, \ldots, T$. The implementation of the method for clustering time series is carried out in three stages: first, the algorithm starts with the estimation of the posterior predictive distributions for each time series, for 25-, 50-, and 100-year return values by means of the approach described in Section 2.1. In order to accommodate features often exhibited by temperature records such as trends or seasonality, the location and scale parameters are allowed to vary in time (in this case, years). Specifically, the location and scale parameters associated with the ith time series are modeled as $\mu_i(t) = \beta_{0,i} + \beta_{1,i}t$. and $\sigma_i(t) = \exp(\gamma_{0,i} + \gamma_{1,i}t)$, respectively, where the exponential function is used to ensure that the positivity of σ is maintained for all values of t. On the other hand, we took a near-flat normal multivariate distribution for $\boldsymbol{\theta}_i := (\beta_{0,i}, \beta_{1,i}, \gamma_{0,i}, \gamma_{1,i}, \xi_i)$ as a prior distribution which reflects the absence of external information. A Markov chain is generated (by means of the Metropolis–Hastings algorithm) of length $N = 10{,}000$, $(\boldsymbol{\theta}_i^{(1)}, \dots, \boldsymbol{\theta}_i^{(N)})$, with $\boldsymbol{\theta}_i^{(j)} := (\beta_{0,i}^{(j)}, \beta_{1,i}^{(j)}, \gamma_{0,i}^{(j)}, \gamma_{1,i}^{(j)}, \xi_i^{(j)})$ for $j = 1, \dots, N$, including a *burn-in* period of 5000 observations with target distribution $\pi(\boldsymbol{\theta}_i|\boldsymbol{x})$ being the initial values the maximum log-likelihood estimates obtained from the distribution of the r-largest order statistic model. Furthermore, only every fifth iteration is stored in order to obtain an independent and identically distributed sample. From the Markov Chain sequence $(\boldsymbol{\theta}_i^{(1)}, \dots, \boldsymbol{\theta}_i^{(n)})$, with $n = 1000$, a sample from the posterior predictive distribution of the return value $x_p^{(i)}$, say, $\mathbf{x}_p^{(i)} := (x_{p,1}^{(i)}, x_{p,2}^{(i)}, \dots, x_{p,n}^{(i)})$ can be generated as follows: let $G^{-1}(\cdot|\boldsymbol{\theta}_i)$ be the inverse of the extreme value distribution in Equation (2) then $x_{p,j}^{(i)} = G^{-1}(1 - p|\boldsymbol{\theta}_i^{(j)})$, for $j = 1, \dots, n$. Thus, an estimate of $F_{x_p^{(i)}}(z|\boldsymbol{x})$ is given by

$$\hat{F}_{x_p^{(i)}}(z|\boldsymbol{x}) := \frac{1}{n}\sum_{j=1}^{n} I(x_{p,j}^{(i)} \leq z), \tag{3}$$

where $I(\cdot)$ represents the indicator function. Next, we compute the dissimilarity matrix $D := (D_{ij})$, $j, i = 1, \dots, T$. To this extend, an adequate metric between univariate distribution functions is required. The choice of this metric should reflect the final goal of the clustering procedure in the sense that the distance captures the discrepancies between predictive distributions of return values. In this case, the weighted L_2-Wasserstein distance between posterior predictive distributions is adopted. This means that the distance between two time series, say, $\mathbf{X}^{(i)}$ and $\mathbf{X}^{(j)}$ is defined as

$$D_{ij} := \int_0^1 (F_{x_p^{(i)}}^{-1}(y|\boldsymbol{x}) - F_{x_p^{(j)}}^{-1}(y|\boldsymbol{x}))^2 y(1-y)\mathrm{d}y, \tag{4}$$

where $F_{x_p^{(i)}}(\cdot|\boldsymbol{x})$ and $F_{x_p^{(j)}}(\cdot|\boldsymbol{x})$ denote the posterior predictive distribution functions of the return values of the ith and jth time series $x_p^{(i)}$ and $x_p^{(j)}$, respectively, with $p = 1/m$, corresponding to a return period of m years. The distances D_{ij} are estimated through the expression

$$\hat{D}_{ij}^2 := \sum_{\ell=1}^{h} (\hat{F}_{x_p^{(i)}}^{-1}(s_\ell|\boldsymbol{x}) -, \hat{F}_{x_p^{(j)}}^{-1}(s_\ell|\boldsymbol{x}))^2 s_\ell(1-s_\ell), \tag{5}$$

where $s_\ell := \ell/(h+1)$, i.e. $(s_1, s_2, \dots, s_h)$ is a regular grid in the interval (0, 1). In the present analysis, we considered $h = 99$. Notice that the expression in Equation (5) is a weighted sum of the squared difference of the estimated percentiles of the returns for the ith series and jth series. Finally, a dendrogram based on the application of classical cluster techniques to the dissimilarity matrix is built and that gives us the different clusters formed by the predictive distributions for 25-, 50- and 100-year return values. In particular, agglomerative hierarchical methods with nearest distance (single linkage), furthest distance (complete linkage) and unweighted average distance (average linkage) are used as grouping criteria.

In the next section, the results obtained by applying the average linkage procedure are presented. Similar conclusions are obtained using the other two methods.

3. Exploring the ECA data set

Time series of daily mean temperature were obtained from the ECA data set [22,23]. Blended data were used in order to have records as complete as possible. Blending consists in infilling gaps with observations from nearby stations (provided that they are within 25 km distance and that height differences are less than 50 m). The data set is subject to quality control procedures, but inhomogeneities can remain (e.g. due to changes in observation practices) and can influence the analysis of extreme temperatures [42].

Stations in western Europe with data from at least January 1901 to December 2007 were selected from the ECA blended data set (note that clustering based on long-term prediction requires time series data ending at the same time). Furthermore, only time series for which the % of missing values is smaller than 2% were considered in the study. Details are displayed in Figure 1 and Table 1.

The method approach described in Section 2 is applied to obtain clusters of the air temperature observations on the basis of 25-, 50- and 100-year return values. Table 2 summarizes the results of the Bayesian analysis, including the r-largest order statistic and the estimates (i.e. mean of the marginal posterior distributions) of the location (μ), scale (σ) and shape (ξ) parameters of the GEV distribution, with the location and scale parameters assumed to evolve in time as $\mu(t) = \beta_0 + \beta_1 t$ and $\sigma(t) = \exp(\gamma_0 + \gamma_1 t)$, respectively.

A closer look at Table 2 reveals that only in Halle, Leipzig, Kyiv, Salzburg and Osijek (HAL, LEI, KYI, SAL and OSI), the assumption of no linear trend in the location parameter is tenable at any conventional level of significance. All stations except Stockholm (STO) and Bremen (BRE) show a positive slope (β_1), indicating an increasing trend in the location parameter. Furthermore, for St Petersburg, Hamburg, Bremen and Bologna (STP, HAM, BRE and BOL), the estimated values of γ_1 indicate non-constant variance. Moreover, note that for all locations the posterior mean for ξ (which plays a key role in determining the tail behavior of the data set underlying distribution) is negative, clearly indicating that a bounded upper tail distribution may be a reasonable choice to fit the data sets corresponding to these locations. A negative value for the shape parameter ξ was also found for daily maximum temperature by Nogaj *et al.* [26] and Parey [27]. At this point, it is important to remind that an immediate advantage of the Bayesian approach is the fact that the entire posterior density of the parameters is constructed, so that the degree of estimation

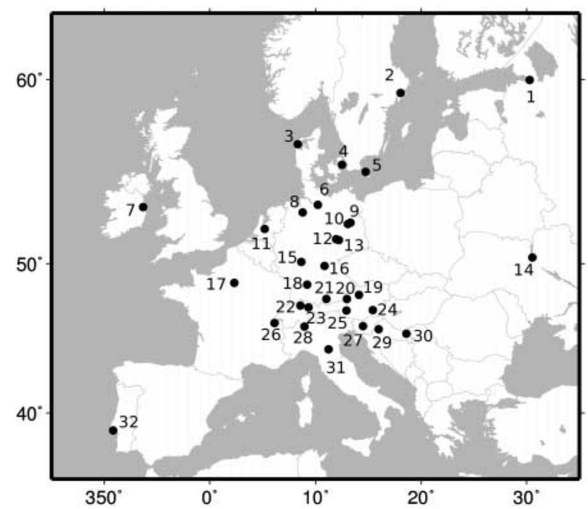

Figure 1. Map showing the location of the analyzed air temperature records. The station numbers are as in Table 1.

Table 1. Summary of the analyzed air temperature records.

	Station (abbreviation)	Longitude	Latitude	% missing values	Height (m)
1	ST. PETERSBURG (STP)	30.3	59.97	0.08	3
2	STOCKHOLM (STO)	18.05	59.35	0	44
3	VESTERVIG (VES)	8.32	56.77	0.04	18
4	KOEBENHAVN (KOE)	12.53	55.68	0.06	9
5	HAMMER ODDE FYR (HOF)	14.78	55.3	0.58	11
6	HAMBURG (HAM)	10.25	53.48	0.75	35
7	DUBLIN (DUB)	353.68	53.35	0.01	49
8	BREMEN (BRE)	8.78	53.05	0.98	5
9	BERLIN (BER)	13.3	52.45	1.51	58
10	POTSDAM (POT)	13.07	52.38	1.51	81
11	DE BILT (DEB)	5.18	52.1	0.05	2
12	HALLE (HAL)	11.98	51.48	0.04	104
13	LEIPZIG (LEI)	12.23	51.43	0	141
14	KYIV (KYI)	30.53	50.4	0.39	166
15	FRANKFURT (FRE)	8.67	50.12	0.27	112
16	BAMBERG (BAM)	10.88	49.88	1.56	239
17	PARIS (PAR)	2.33	48.82	0.01	75
18	STUTTGART (STU)	9.22	48.72	0.33	401
19	KREMSMUENSTER (KRE)	14.13	48.05	0.12	383
20	SALZBURG (SAL)	13	47.8	1.89	437
21	HOHENPEISSENBERG (HOH)	11.02	47.8	1.68	977
22	ZUERICH (ZUE)	8.57	47.38	0.21	556
23	SAENTIS (SAE)	9.35	47.25	0.25	2490
24	GRAZ (GRA)	15.45	47.08	0.52	366
25	SONNBLICK (SON)	12.95	47.05	0.08	3106
26	GENEVE (GEN)	6.13	46.25	0.26	405
27	LJUBLJANA BEZIGRAD (LJU)	14.52	46.05	1.1	299
28	LUGANO (LUG)	8.97	46	0.25	273
29	ZAGREB-GRIC (ZAG)	15.97	45.82	0.07	156
30	OSIJEK (OSI)	18.63	45.53	0.82	88
31	BOLOGNA (BOL)	11.25	44.48	0.15	53
32	LISBOA (LIS)	350.85	38.72	0.05	77

uncertainty can be quantified. As an illustrative example, we display in Figure 2 the posterior density estimates of ξ in Bamberg (BAM).

A common feature of the posterior distributions associated with the shape parameter, for all the 32 stations, is that the probability of non-negative values for ξ is negligible clearly indicating that a bounded upper tail distribution may be a reasonable choice to fit the data sets corresponding to these locations. A bounded upper tail distribution is not only reasonable from the statistical point of view but also from a physical perspective, in the sense that thermodynamic considerations lead to a upper limit to Earth's air temperature.

Some considerations of practical order are required at this point. In order to generate a sample $(x^{(i)}_{p,t,0}, \ldots, x^{(i)}_{p,t,n})$ from the posterior predictive distribution of the return value $x^{(i)}_{p,t}$ for 25-, 50- and 100-years, associated with the ith time series ($i = 1, \ldots, 32$), we proceed as follows: first, from the Markov Chain sequence $(\boldsymbol{\theta}^{(1)}_i, \ldots, \boldsymbol{\theta}^{(n)}_i)$ calculate the values $\mu_{i,j}(t) = \beta^{(j)}_{0,i} + \beta^{(j)}_{1,i} t^*$ and $\sigma_{i,j}(t) = \exp(\gamma^{(j)}_{0,i} + \gamma^{(j)}_{1,i} t^*)$, for $j = 1, \ldots, n$, being $t^* = (t - 1954)/53$ with $t = 2032, 2057$ and 2107 corresponding to $p = 0.04, 0.02$ and 0.01, respectively. Second, compute $x^{(i)}_{p,t,j} := \mu_{i,j}(t) - \sigma_{i,j}(t) \log\{-\log(1-p)\}$ if $\xi^{(j)}_i \approx 0$, or

$$x^{(i)}_{p,t,j} := \mu_{i,j}(t) - \frac{\sigma_{i,j}(t)}{\xi^{(j)}_i}\{1 - (-\log(1-p))^{-\xi^{(j)}_i}\},$$

otherwise.

Table 2. r-Largest order statistics, parameters estimates and posterior standard deviations (in parentheses).

Location	r	$\hat{\beta}_0$	$\hat{\beta}_1$	$\hat{\gamma}_0$	$\hat{\gamma}_1$	$\hat{\xi}$
STP	7	25.46 (0.08)	0.73 (0.18)	0.25 (0.02)	0.29 (0.06)	−0.38 (0.05)
STO	6	23.23 (0.07)	−1.13 (0.23)	0.29 (0.02)	0.13 (0.06)	−0.31 (0.04)
VES	5	22.18 (0.10)	1.94 (0.31)	0.35 (0.02)	0.06 (0.09)	−0.27 (0.06)
KOE	5	23.28 (0.08)	1.66 (0.28)	0.19 (0.02)	0.15 (0.09)	−0.29 (0.07)
HOF	5	22.26 (0.09)	1.56 (0.31)	0.32 (0.02)	0.26 (0.09)	−0.19 (0.03)
HAM	7	24.85 (0.09)	1.32 (0.30)	0.30 (0.02)	0.47 (0.07)	−0.32 (0.06)
DUB	9	19.90 (0.06)	0.94 (0.21)	−0.09 (0.02)	−0.09 (0.07)	−0.22 (0.04)
BRE	8	25.80 (0.09)	−0.76 (0.31)	0.35 (0.02)	−0.42 (0.08)	−0.42 (0.07)
BER	7	25.96 (0.08)	0.68 (0.29)	0.15 (0.02)	0.14 (0.08)	−0.31 (0.08)
POT	5	25.82 (0.09)	1.39 (0.32)	0.25 (0.02)	0.17 (0.09)	−0.31 (0.03)
DEB	5	24.21 (0.11)	1.14 (0.36)	0.31 (0.03)	−0.09 (0.11)	−0.30 (0.05)
HAL	7	26.14 (0.09)	0.10 (0.38)	0.23 (0.02)	0.03 (0.09)	−0.29 (0.02)
LEI	6	26.21 (0.10)	0.51 (0.38)	0.26 (0.02)	0.13 (0.10)	−0.31 (0.06)
KYI	7	26.84 (0.09)	0.17 (0.32)	0.23 (0.03)	0.06 (0.08)	−0.25 (0.07)
FRE	5	26.25 (0.09)	1.81 (0.27)	0.24 (0.03)	0.17 (0.09)	−0.24 (0.04)
BAM	5	24.93 (0.10)	1.18 (0.37)	0.27 (0.04)	0.07 (0.12)	−0.16 (0.03)
PAR	7	27.00 (0.11)	2.18 (0.32)	0.37 (0.03)	0.19 (0.08)	−0.23 (0.08)
STU	7	25.11 (0.10)	1.00 (0.30)	0.23 (0.03)	−0.04 (0.10)	−0.23 (0.05)
KRE	7	24.40 (0.07)	0.65 (0.21)	0.10 (0.03)	−0.11 (0.07)	−0.24 (0.05)
SAL	8	26.28 (0.08)	0.23 (0.17)	0.21 (0.02)	−0.17 (0.07)	−0.45 (0.06)
HOH	9	23.27 (0.10)	1.62 (0.31)	0.26 (0.03)	0.06 (0.07)	−0.23 (0.05)
ZUE	7	24.63 (0.08)	1.31 (0.29)	0.10 (0.04)	0.04 (0.10)	−0.26 (0.03)
SAE	7	13.43 (0.10)	1.90 (0.38)	0.24 (0.03)	−0.03 (0.10)	−0.25 (0.06)
GRA	7	24.91 (0.07)	3.00 (0.25)	0.02 (0.03)	0.06 (0.09)	−0.20 (0.05)
SON	5	8.19 (0.08)	2.37 (0.25)	0.09 (0.03)	−0.13 (0.09)	−0.23 (0.06)
GEN	7	25.80 (0.09)	0.91 (0.32)	0.19 (0.03)	0.01 (0.09)	−0.23 (0.05)
LJU	5	25.75 (0.10)	2.41 (0.29)	0.12 (0.03)	0.06 (0.12)	−0.19 (0.02)
LUG	7	26.18 (0.07)	0.76 (0.23)	−0.08 (0.03)	−0.08 (0.09)	−0.23 (0.07)
ZAG	7	27.93 (0.07)	0.56 (0.21)	0.10 (0.02)	−0.04 (0.07)	−0.23 (0.04)
OSI	7	28.01 (0.08)	0.07 (0.28)	0.10 (0.03)	−0.15 (0.10)	−0.26 (0.08)
BOL	5	30.43 (0.06)	0.46 (0.18)	0.10 (0.02)	−0.20 (0.07)	−0.26 (0.04)
LIS	5	29.71 (0.10)	1.17 (0.33)	0.27 (0.03)	0.20 (0.11)	−0.24 (0.08)

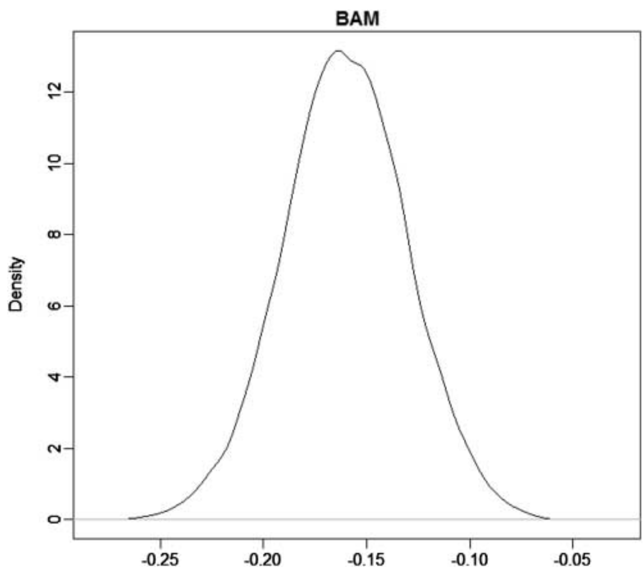

Figure 2. Marginal posterior distribution for the shape parameter ξ in Bamberg (BAM).

Table 3. Bayesian estimates for the return values of 25, 50 and 100 years.

	Return values		
	25	50	100
STP	29.66 (0.34)	30.13 (0.39)	30.69 (0.45)
STO	25.13 (0.20)	25.21 (0.22)	25.93 (0.31)
VES	25.10 (0.24)	25.52 (0.27)	26.14 (0.34)
KOE	26.96 (0.11)	27.48 (0.14)	28.27 (0.18)
HOF	28.60 (0.63)	29.83 (0.82)	31.69 (1.23)
HAM	31.26 (0.57)	32.09 (0.65)	31.89 (0.59)
DUB	23.10 (0.26)	23.58 (0.31)	24.19 (0.40)
BRE	26.58 (0.42)	26.61 (0.50)	27.10 (0.79)
BER	28.54 (0.36)	28.87 (0.42)	29.30 (0.52)
POT	29.10 (0.40)	29.55 (0.46)	30.23 (0.60)
DEB	28.40 (0.45)	29.00 (0.53)	29.80 (0.70)
HAL	28.76 (0.15)	29.08 (0.21)	29.33 (0.30)
LEI	28.36 (0.13)	29.16 (0.15)	29.40 (0.19)
KYI	29.62 (0.14)	29.98 (0.15)	30.28 (0.17)
FRE	31.74 (0.42)	32.54 (0.50)	33.71 (0.62)
BAM	29.60 (0.48)	30.35 (0.56)	31.28 (0.72)
PAR	32.95 (0.42)	33.91 (0.50)	35.30 (0.69)
STU	29.23 (0.39)	29.87 (0.45)	30.69 (0.59)
KRE	27.61 (0.27)	28.06 (0.31)	28.59 (0.40)
SAL	28.00 (0.14)	28.08 (0.17)	28.22 (0.20)
HOH	28.12 (0.37)	28.85 (0.43)	29.85 (0.55)
ZUE	28.63 (0.38)	29.24 (0.45)	30.10 (0.60)
SAE	18.56 (0.48)	19.37 (0.57)	20.56 (0.74)
GRA	30.86 (0.33)	31.83 (0.38)	33.37 (0.49)
SON	13.51 (0.31)	14.34 (0.36)	15.62 (0.47)
GEN	29.67 (0.41)	30.26 (0.48)	31.02 (0.63)
LJU	31.44 (0.36)	32.41 (0.43)	33.96 (0.56)
LUG	29.22 (0.30)	29.68 (0.35)	30.29 (0.49)
ZAG	31.07 (0.25)	31.52 (0.29)	32.00 (0.36)
OSI	30.41 (0.10)	30.72 (0.12)	30.98 (0.17)
BOL	33.33 (0.21)	33.69 (0.25)	34.06 (0.29)
LIS	34.08 (0.41)	34.73 (0.51)	35.62 (0.64)

Note: Posterior standard deviations in parenthesis.

Table 3 presents predictive return values estimates (i.e. mean of the predictive distributions) for 25-, 50- and 100-years, including posterior standard deviations. Return values can be interpreted as the daily mean temperature value that is expected to be exceeded on average once every return period, or with probability 1/(return period) in any given year.

For a spatial interpretation of the estimated return levels, time-series clustering is applied as described in Section 2. The results of the clustering procedure are illustrated by a tree diagram usually referred to as *dendrogram*, which represents the arrangement of the clusters produced by hierarchical agglomerative clustering. In Figures 3–5, dendrograms based on average linkage obtained for 25-, 50- and 100-year horizons are displayed. The vertical axis represents the distance at which two clusters are joined.

As previously mentioned, the results obtained by the three clustering approaches are in general similar, particularly for the complete and average linkage methods. The largest distance between stations distinguishes a cluster with Saentis (SAE) and Sonnblick (SON) from the remaining locations. These are the highest altitude stations at 2490 and 3106 m, respectively, with the lowest 25-year return values. The second largest distance discriminates mainly the northern stations with maritime climate or on the continental-maritime boundary (STO, VES, KOE, BRE, DUB) from the remaining stations in central and southern Europe. Within this large remaining cluster

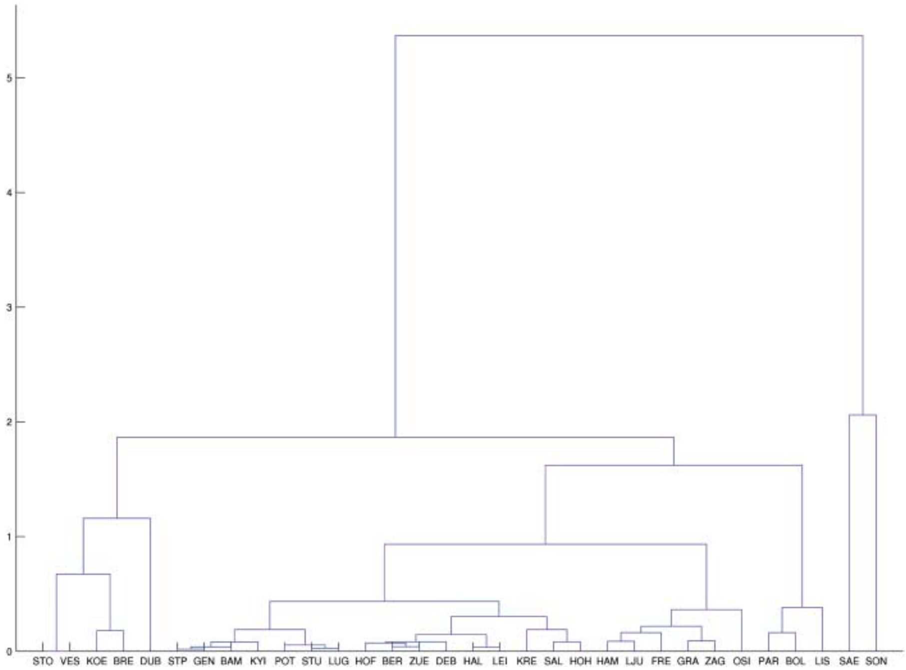

Figure 3. Dendrogram for 25-year return values based on the average linkage method.

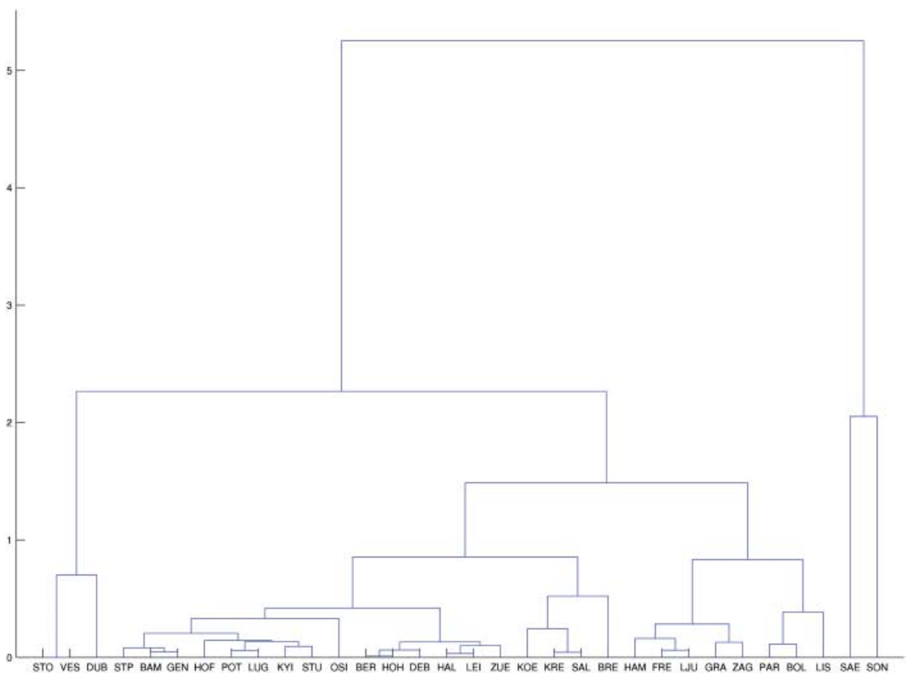

Figure 4. Dendrogram for 50-year return values based on the average linkage method.

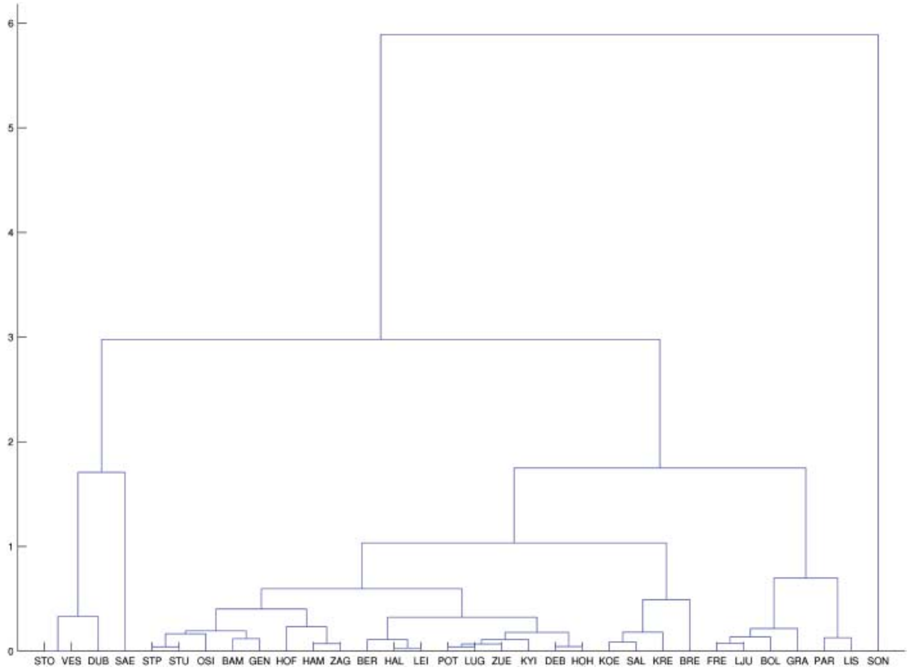

Figure 5. Dendrogram for 100-year return values based on the average linkage method.

of European stations, there is a further discrimination between roughly northern and southern stations, with a further distinction between the south-eastern stations and the more western (Paris, Bologna and Lisbon) locations.

4. Conclusions

In this work, a Bayesian extreme value analysis has been carried out for deriving the distributions of return period from long series of daily mean temperature over Europe. The extreme value analysis has been further combined with a time-series clustering procedure in order to obtain a description of the relationship between return values at different sites. One of the clear advantages of the approach applied in this work is that clustering is performed on the distribution of return values rather than on the return values themselves, enabling a more complete description of temperature extremes and corresponding uncertainties.

At most stations, the location parameter of the data distribution exhibits a statistically significant increasing (linear) trend. Trends in temperature extremes over Europe are thought to be associated with changes in large-scale circulation and corresponding weather patterns [12,13,43] and likely also to changes in snow cover extent over Europe [5].

Clustering of the estimated distributions of return values yields clusters of stations reflecting spatial consistency over Europe at regional scales. The analysis identifies the highest altitude stations (Saentis and Sonnblick) as the most different from the remaining group of stations in terms of the distribution of return periods. A clear distinction is also found between the northernmost stations in Scandinavia, and the stations in central and southern Europe. This spatial structure of the return period distributions seems to be consistent with projected changes in the variability of temperature extremes over Europe pointing to a different behavior in central Europe than in northern Europe and the Mediterranean area, possibly related to the effect of soil moisture and land–atmosphere coupling [15].

Statistical approaches dealing with the complete data distribution, such as the Bayesian extreme value analysis applied in the present study, are particularly appealing for the analysis of climate time series, considering the importance of changes in variability rather than in the mean, specially in the context of temperature extremes and climate change. Further extensions of the present work would include the analysis of data outputs from regional climate models using the the Bayesian methodology described in this study.

Acknowledgements

The authors would like to express their gratitude to two anonymous referees for all helpful comments and constructive criticism. The three authors are supported by 'Acções Integradas Luso-Espanholas' under the grants E-83/09 and HP2008-008. The third author also acknowledges the support of grant SEJ2007-64500.

References

[1] L.V. Alexander, X. Zhang, T.C. Peterson, J. Caesar, B. Gleason, A.M.G. Klein Tank, M. Haylock, D. Collins, B. Trewin, F. Rahimzadeh, A. Tagipour, K. Rupa Kumar, J. Revadekar, G. Griffiths, L. Vincent, D.B. Stephenson, J. Burn, E. Aguilar, M. Brunet, M. Taylor, M. New, P. Zhai, M. Rusticucci, and J.L. Vazquez-Aguirre, *Global observed changes in daily climate extremes of temperature and precipitation*, J. Geophys. Res. 111 (2006), p. D05109.

[2] R. Basu and J.M. Samet, *Relation between elevated ambient temperature and mortality: A review of the epidemiologic evidence*, Epidemiol. Rev. 24 (2002), pp. 190–202.

[3] M. Beniston, *The 2003 heat wave in Europe: A shape of things to come? An analysis based on Swiss climatological data and model simulations*, Geophys. Res. Lett. 31 (2004), p. L02202.

[4] M. Beniston, D.B. Stephenson, O.B. Christensen, C.A.T. Ferro, C. Frei, S. Goyette, K. Halsnaes, T. Holt, K. Jylha, B. Koffi, J. Palutikof, R. Schoell, T. Semmler, and K. Woth, *Future extreme events in European climate: An exploration of regional climate model projections*, Climatic Change 81 (2007), pp. 71–95.

[5] E.J.M. van den Besselaar, A.M.G. Klein Tank, and G. van der Schrier, *Influence of circulation types on temperature extremes in Europe*, Theor. Appl. Climatol. 99 (2010), pp. 431–439.

[6] T. Buishand, L. de Haan, and C. Zhou, *On spatial extremes: With application to a rainfall problem*, Ann. Appl. Statist. 2 (2008), pp. 624–642.

[7] G. Choi, D. Collins, G. Ren, B. Trewin, M. Baldi, Y. Fukuda, M. Afzaal, T. Pianmana, P. Gomboluudev, P.T.T. Huong, N. Lias, W.T. Kwon, K.O. Boo, Y.M. Cha, and Y. Zhou, *Changes in means and extreme events of temperature and precipitation in the Asia-Pacific network region*, Int. J. Climatol. 29 (2007), pp. 1906–1925.

[8] N. Christidis, P.A. Stott, S. Brown, G.C. Hegerl, and J. Caesar, *Detection of changes in temperature extremes during the second half of the 20th century*, Geophys. Res. Lett. 32 (2005), p. L20716.

[9] D. Cooley, *Extreme value analysis and the study of climate change*, Climatic Change 97 (2009), pp. 77–83.

[10] D. Cooley, P. Naveau, and P. Poncet, *Variograms for spatial max-stable random fields*, in *Dependence in Probability and Statistics*, Lectures Notes in Statistics, Springer, New York, 2006, pp. 373–390.

[11] D. Cooley, D. Nychka, and P. Naveau, *Bayesian spatial modeling of extreme precipitation return levels*, J. Amer. Statist. Assoc. 102 (2007), pp. 824—-840.

[12] P.M. Della-Marta, M.R. Haylock, J. Luterbacher, and H. Wanner, *Doubled length of western European summer heat waves since 1880*, J. Geophys. Res. 112 (2007), p. D15103.

[13] P. Domonkos, J. Kysely, K. Piotrowicz, P. Petrovic, and T. Likso, *Variability of extreme temperature events in South-Central Europe during the 20th century and its relationship with large-scale circulation*, Int. J. Climatol. 23 (2003), pp. 987–1010.

[14] A.H. Fink, T. Brücher, G.C. Leckebusch, A. Krüger, J.G. Pinto, and U. Ulbrich, *The 2003 European summer heatwaves and drought – synoptic diagnosis and impacts*, Weather 59 (2004), pp. 209–216.

[15] E.M. Fischer and C. Schär, *Future changes in daily summer temperature variability: Driving processes and role for temperature extremes*, Clim. Dynam. 33 (2009), pp. 917–935.

[16] P. Frich, L.V. Alexander, P.M. Della-Marta, B. Gleason, M. Haylock, A.M.G. Klein Tank, and T. Peterson, *Observed coherent changes in climatic extremes during the second half of the twentieth century*, Climate Res. 19 (2002), pp. 193–212.

[17] W.M. Jolly, M. Dobbertin, N.E. Zimmermann, and M. Reichstein, *Divergent vegetation growth responses to the 2003 heat wave in the Swiss Alps*, Geophys. Res. Lett. 32 (2005), p. L18409.

[18] T.R. Karl and R.G. Quayle, *The 1980 summer heat-wave and drought in historical perspective*, Mon. Weather Rev. 109 (1981), pp. 2055–2073.

[19] R.W. Katz and B.G. Brown, *Extreme events in a changing climate: Variability is more important than averages*, Climatic Change 21 (1992), pp. 289–302.
[20] V. Kharin and F. Zwiers, *Estimating extremes in transient climate change simulations*, J. Climate 18 (2005), pp. 1156–1173.
[21] A.M.G. Klein Tank and G.P. Können, *Trends in indices of daily temperature and precipitation extremes in Europe, 1946–1999*, J. Climate 16 (2003), pp. 3665–3680.
[22] A.M.G. Klein Tank, J.B. Wijngaard, G.P. Können, R. Böhm, G. Demarée, A. Gocheva, M. Mileta, S. Pashiardis, L. Hejkrlik, C. Kern-Hansen, R. Heino, P. Bessemoulin, G. Müller-Westermeier, M. Tzanakou, S. Szalai, T. Pálsdóttir, D. Fitzgerald, S. Rubin, M. Capaldo, M. Maugeri, A. Leitass, A. Bukantis, R. Aberfeld, A.F.V. van Engelen, E. Forland, M. Mietus, F. Coelho, C. Mares, V. Razuvaev, E. Nieplova, T. Cegnar, J.A. López, B. Dahlström, A. Moberg, W. Kirchhofer, A. Ceylan, O. Pachaliuk, L.V. Alexander, and P. Petrovic, *Daily dataset of 20th century surface air temperature and precipitation series for the European climate assessment*, Int. J. Climatol. 22 (2002), pp. 1441–1453.
[23] E.J. Klok and A.M.G. Klein Tank, *Updated and extended European dataset of daily climate observations*, Int. J. Climatol. 29 (2009), pp. 1182–1191.
[24] G.A. Meehl, K.T. Easterling, S. Changnon, R. Pielke, D. Changnon, J. Evans, P.Y. Groisman, T.R. Knutson, K.E. Kunkel, L.O. Mearns, C. Parmesan, R. Pulwarty, T. Root, R.T. Sylves, P. Whetton, and F. Zwiers, *An introduction to trends in extreme weather and climate events: observations, socioeconomic impacts, terrestrial ecological impacts, and model projections*, Bull. Am. Meteorol. Soc. 81 (2000), pp. 413–416.
[25] A. Moberg and P.D. Jones, *Trends in indices for extremes in daily temperature and precipitation in central and western Europe, 1901–1999*, Int. J. Climatol. 25 (2005), pp. 1149–1171.
[26] M. Nogaj, P. Yiou, S. Parey, F. Malek, and P. Naveau, *Amplitude and frequency of temperature extremes over the North Atlantic region*, Geophys. Res. Lett. 33 (2206), p. L10801.
[27] S. Parey, *Extremely high temperatures in France at the end of the century*, Climate Dyn. 30 (2008), pp. 99–112.
[28] J.A. Patz, D. Campbell-Lendrum, T. Holloway, and J.A. Foley, *Impact of regional climate change on human health*, Nature 438 (2005), pp. 310–317.
[29] T.C. Peterson, *Climate change indices*, World Meteorol. Org. Bull. 54 (2005), pp. 83–86.
[30] S. Planton, M. Deque, F. Chauvin, and L. Terray, *Expected impacts of climate change on extreme climate events*, C.R. Geosci. 340 (2008), pp. 564–574.
[31] R.D. Reiss and M. Thomas, *Statistical Analysis of Extreme Values: With Applications to Insurance, Finance, Hydrology and Other Fields*, Birkhäuser, Basel, 2007.
[32] S.M. Robeson and J.A. Doty, *Identifying rogue air temperature stations using cluster analysis of percentile trends*, J. Climate 18 (2005), pp. 1275–1287.
[33] H. Sang and A.E. Gelfand, *Hierarchical modeling for extreme values observed over space and time*, Environ. Ecol. Stat. 16 (2009), pp. 407–426.
[34] H. Sang and A.E. Gelfand, *Continuous spatial process models for spatial extreme values*, J. Agric. Biol. Environ. Stat. 15 (2010), pp. 49–65.
[35] C. Schär, P.L. Vidale, D. Luthi, C. Frei, C. Haberli, M.A. Liniger, and C. Appenzeller, *The role of increasing temperature variability in European summer heatwaves*, Nature 427 (2004), pp. 332–336.
[36] M.G. Scotto, A.M. Alonso, and S.M. Barbosa, *Clustering time series of sea levels: Extreme value approach*, J. Waterway, Port, Coastal, and Ocean Engrg. 136 (2010), pp. 215–225.
[37] C. Tebaldi, K. Hayhoe, J.M. Arblaster, and G.A. Meehl, *Going to the extremes – an intercomparison of model-simulated historical and future changes in extreme events*, Climatic Change 79 (2006), pp. 185–211.
[38] G. Theoharatos, K. Pantavou, A. Mavrakis, A. Spanou, G. Katavoutas, P. Efstathiou, P. Mpekas, and D. Asimakopoulos, *Heat waves observed in 2007 in Athens, Greece: Synoptic conditions, bioclimatological assessment, air quality levels and health effects*, Environ. Res. 110 (2010), pp. 152–161.
[39] A. Toreti and F. Desiato, *Changes in temperature extremes over Italy in the last 44 years*, Int. J. Climatol. 28 (2008), pp. 733–745.
[40] R.M. Trigo, J.M.C. Pereira, M.G. Pereira, B. Mota, T.J. Calado, C.C. Dacamara, and F.E. Santo, *Atmospheric conditions associated with the exceptional fire season of 2003 in Portugal*, Int. J. Climatol. 26 (2006), pp. 1741–1757.
[41] T.M.L. Wigley, *The effect of changing climate on the frequency of absolute extreme events*, Climate Monit. 17 (1988), pp. 44–55.
[42] J.B. Wijngaard, A.M.G. Klein Tank, and G.P. Können, *Homogeneity of 20th century European daily temperature and precipitation series*, Int. J. Climatol. 23 (2003), pp. 679–692.
[43] P. Yiou and M. Nogaj, *Extreme climatic events and weather regimes over the North Atlantic: When and where?* Geophys. Res. Lett. 31 (2004), p. L07202.
[44] B.F. Zaitchik, A.K. Macalady, L.R. Bonneau, and R.B. Smith, *Europe's 2003 heat wave: A satellite view of impacts and land-atmosphere feedbacks*, Int. J. Climatol. 26 (2006), pp. 743–769.